

UDK: 612.086.3; 622.785; 676.017.2; 669.018.29

## **Performances of Vermiculite and Perlite Based Thermal Insulation Lightweight Concretes**

**Anja Terzić<sup>1\*</sup>\*, Jovica Stojanović<sup>2</sup>, Ljubiša Andrić<sup>2</sup>, Ljiljana Miličić<sup>1</sup>, Zagorka Radojević<sup>1</sup>**

<sup>1</sup>Institute for Testing of Materials - IMS, Vojvode Mišića Bl. 43, 11000 Belgrade, Serbia

<sup>2</sup>Institute for Technology of Nuclear and other Mineral Raw Materials, Franchet d'Esperey 86, 11000 Belgrade, Serbia

---

### **Abstract:**

*This experimental study was conducted with an aim to investigate the effect of the elevated temperature on the mineral phase composition, microstructure and mechanical properties of the thermal insulation lightweight concretes. The first group of experimental concretes was based on the expanded vermiculite and expanded perlite used as lightweight aggregates (in 65 wt%) in combination with either ordinary Portland cement or refractory calcium aluminate cement. The mix-design of the second group of concretes comprised standard quartz aggregate, vermiculite or perlite as aggregate replacement (25 wt%) and binder (PC or CAC). A total of 10 concrete mix-designs were fabricated in form of 40×40×160 mm samples which were submitted to heat-treatment at 400°, 600°, 800° and 1000 °C upon standard 28-days period of curing and hardening. The changes in crystallinity and mineral phase composition induced by temperature were monitored by X-ray diffraction technique. Microstructural visualizations of the non-fired and fired concrete samples were conducted by scanning electron microscopy accompanied with EDX analysis. The results indicated that despite the decrease in compressive strengths upon firing, investigated lightweight concretes can be categorized both as thermal insulators and structural materials.*

**Keywords:** Sintering; Mineral phase composition; SEM; Mechanical properties, Construction materials.

---

## **1. Introduction**

Modern civil engineering is continuously imposing new requests regarding the reduction in the weight of structural elements, as well as energy-efficiency and fire safety [1-3]. One of the solutions for these demands is the application of the lightweight concretes. These materials are characterized by low density and low thermal conductivity; and thereby a good thermal insulation [4-7]. Apart from suitable thermal characteristics, lightweight concretes are often designed with available and affordable raw materials of primary or secondary origin (e.g. expanded clay or vermiculite, perlite, pumice, coal ash, etc.) which places them in group of low-cost building materials [8, 9].

Aggregates characterized by specific weight less than 1120 kg/m<sup>3</sup> are generally considered as lightweight resources for the concrete production [3]. Vermiculite and perlite

---

\* Corresponding author: [anja.terzic@institutims.rs](mailto:anja.terzic@institutims.rs)

are among the most frequently used lightweight aggregates in civil engineering. Vermiculite as a mica-like mineral with shiny “flakes” is formed during biotite hydrothermal alternation or phlogopite weathering [10]. It belongs to the phyllosilicate group of minerals. The lamellar structure enables its lubricating properties which are being manifested at high temperatures. Thereby, vermiculite can be used as fireproof material or as lightweight porous filler for heat insulating [11, 12]. The chemical composition of vermiculite is not altering during the thermal expansion (only chemically bonded water is removed). The bulk density of thermally expanded vermiculite is at least 10 times smaller than its original volume, its thermal conductivity is low (0.04–0.12 W/mK) and melting point is relatively high (1240–1430 °C) [13]. Perlite is amorphous siliceous volcanic glass which is usually formed during obsidian hydration. Perlite has relatively high water content and its volume can significantly expand under the effect of heat [14]. Upon heating above 870 °C, the volume of perlite can increase 4 to 20 times of its original volume. As a consequence, the expanded perlite is characterized by porous structure, high water absorption, low density and good thermal insulation [15-17].

The extensive studies of the application of vermiculite and perlite in various building composites highlighted that these raw materials have certain advantages as well as disadvantages. For instance, the expended vermiculite used in 30-60 % replacement levels contributed to the heat resistance and thermal stability of the cement mortar, despite the increase in water absorption and compressive strength deterioration [18]. Gypsum plasters with the addition of 10 and 20 % expanded vermiculite also exhibited decrease in the 28 days compressive strength; however the 28 days bending strength increased 16 and 35 %, respectively[19]. The addition of vermiculite in plasters led to a reduction in the Young's modulus [20]. Also, 55 % reduction in the compressive strength of clay bricks upon firing at 900 °C was induced by the 10 % addition of vermiculite [21]. The compressive strengths of concretes were reduced as the replacement levels of natural sand with vermiculite increased from 5 to 10 % [22-24]. Similar effect occurred in self-compacting mortars for high-temperature application when 10, 20, 30 and 40 % of raw vermiculite was incorporated in the mix-design [25]. Vermiculite is often being mixed with other types of light-weight aggregates such as polystyrene [26], or combined with geopolymers to create lightweight composite panels with improved thermal properties [27]. Similar to vermiculite addition, the expanded perlite (10 %) combined with 20 % of natural pozzolan improved the mechanical properties of concrete, while 10 % of pozzolan and 10 % of the perlite led to a reduction in the rate of NaCl corrosion [28]. Lightweight geopolymers with fly ash, pumice and perlite produced compressive strengths up to 10-50 MPa as their unit weights changed between 1250 and 1700 kg/m<sup>3</sup> [29]. Thermal conductivity and the over-all durability of concretes were substantially improved with the use of perlite [30-32].

In this study, the properties of thermal insulation concretes have been investigated. Expanded vermiculite and perlite were used as lightweight aggregates in a high percentage (65 wt%) in the mix-design of concretes. Ordinary Portland cement and refractory calcium aluminate cement were alternated as binders. Thus prepared composite building materials were compared with another group of thermal insulation concretes in which standard quartz sand has been replaced by either vermiculite or perlite (in 25 wt%). The changes in physico-mechanical properties, mineral composition and microstructure of the designed concretes were monitored in the thermal range from 20° to 1000 °C.

## **2. Materials and Experimental Procedures**

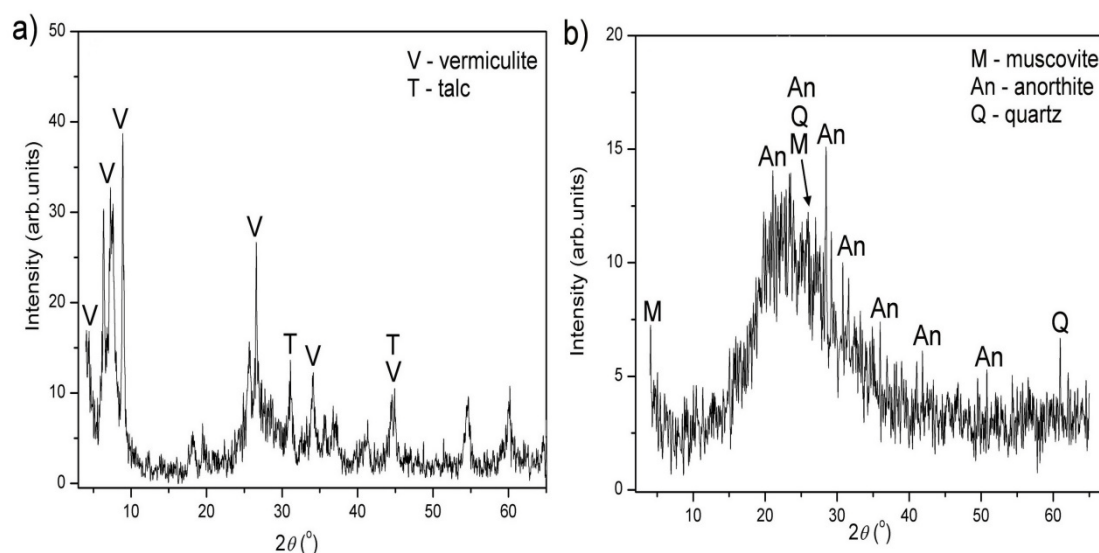
### **2.1. Raw materials**

Perlite and vermiculite were alternated as aggregates in the thermal insulation concretes. The grain-size distributions obtained by dry sieve analysis are given in Tab. I:

**Tab. I** Grain-size distributions of perlite and vermiculite aggregate.

Size class	Vermiculite	Perlite
+5 (mm)	0.37 (wt%)	0.34 (wt%)
- 5 + 0.3 (mm)	92.85 (wt%)	96.54 (wt%)
-0.3 +0 (mm)	6.78 (wt%)	3.13 (wt%)

Chemical compositions of a) perlite:  $\text{SiO}_2=74.4\%$ ,  $\text{Al}_2\text{O}_3=15.4\%$ ,  $\text{Fe}_2\text{O}_3=1.3\%$ ,  $\text{MgO}=0.13\%$ ,  $\text{K}_2\text{O}=4.55\%$ ,  $\text{Na}_2\text{O}=3.38\%$ ; and b) vermiculite:  $\text{SiO}_2=41.2\%$ ,  $\text{Al}_2\text{O}_3=14.94\%$ ,  $\text{CaO}=3.95\%$ ,  $\text{Fe}_2\text{O}_3=7.2\%$ ,  $\text{MgO}=25.5\%$ ,  $\text{K}_2\text{O}=5.1\%$ ,  $\text{TiO}_2=1.4\%$ . Mineral compositions of vermiculite and perlite are provided in Fig 1.

**Fig. 1.** XRD analysis of: a) vermiculite; b) perlite.

Vermiculite (Fig. 1a) was identified in proportions larger than 90 % represented by its high layer stacking, i.e. intense reflections appearing in series between  $2^\circ$  and  $11^\circ$ . The reflections located at  $28^\circ$ , and  $36^\circ$ ,  $48^\circ$  are also characteristic for vermiculite mineral [13]. Talc was present around  $31^\circ$  and  $48^\circ$ . Smectite and chlorite were present in traces. Perlite sample was highly amorphous, which is in agreement with the literature [16]. The only detected crystalline phases were muscovite, anorthite and quartz.

Thermally induced behavior of the raw materials was monitored by differential thermal analysis (Fig. 2).

Both raw materials showed similar exothermic peaks above  $500\text{ }^\circ\text{C}$ , i.e. vermiculite at  $557\text{ }^\circ\text{C}$  (Fig. 2a) and perlite at  $552\text{ }^\circ\text{C}$  (Fig. 2b). The second exothermic effect appeared at  $1023\text{ }^\circ\text{C}$ . It is followed by a steep decreasing curve-line, meaning that both vermiculite and perlite were thermally stable up to  $1000\text{ }^\circ\text{C}$ .

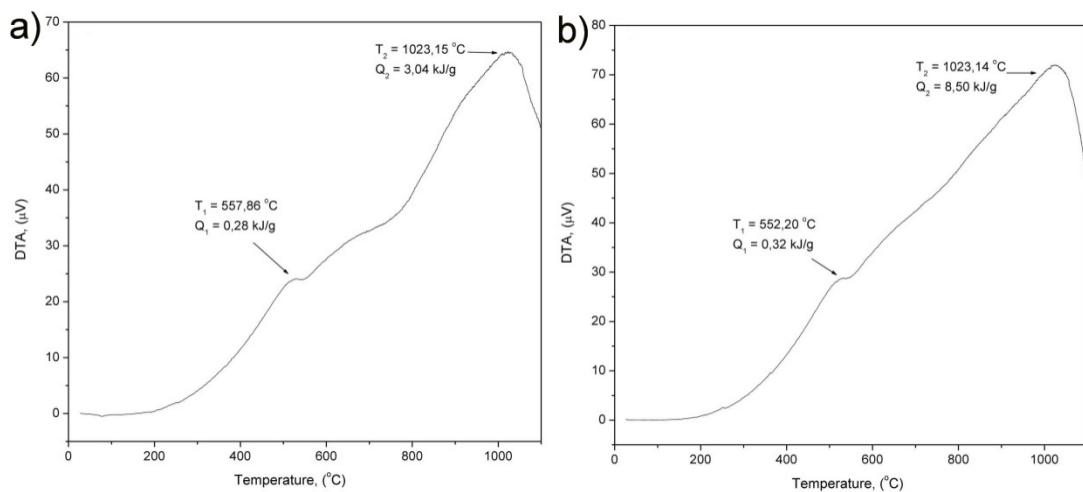


**Fig. 2.** DTA analysis of: a) vermiculite; b) perlite.

## 2.2. Preparation of the experimental samples

Ten concretes prepared for the experiment were based on Portland cement (PC; CEM I 42.5R, Lafarge) or calcium aluminate cement (CAC; Istra 40, Calucem). PC comprised the following oxides:  $\text{SiO}_2 = 21.82\%$ ,  $\text{Al}_2\text{O}_3 = 6.59\%$ ,  $\text{CaO} = 62.36\%$ ,  $\text{Fe}_2\text{O}_3 = 4.75\%$ ,  $\text{MgO} = 2.17\%$ ,  $\text{K}_2\text{O} = 0.78\%$  and  $\text{Na}_2\text{O} = 0.19\%$ . The chemical composition of CAC was as follows:  $\text{SiO}_2 = 3.85\%$ ,  $\text{Al}_2\text{O}_3 = 40.35\%$ ,  $\text{CaO} = 37.50\%$ ,  $\text{Fe}_2\text{O}_3 = 16.28\%$ ,  $\text{MgO} = 0.96\%$ ,  $\text{K}_2\text{O} = 0.15\%$ ,  $\text{Na}_2\text{O} = 0.08\%$  and  $\text{MnO} = 0.2\%$ . Quartz sand ( $\text{SiO}_2 = 98\%$ ; characteristics according to DIN EN 191-1; Überwacht FMPA, Baden Wurtenberg), vermiculite and perlite were alternated as aggregates. The mix designs are provided in Tab. II.

**Tab. II** Mix-designs of the experimental concretes.

Sample	PC (%)	CAC (%)	Quartz sand (%)	Vermiculite (%)	Perlite (%)
PCC	25		65	-	-
CACC		25	65	-	-
PC-P65	25	-	-	-	65
PC-V65	25	-	-	65	-
CAC-P65	-	25	-	-	25
CAC-V65	-	25	-	65	-
PC-Q-P25	25	-	30	-	25
PC-Q-V25	25	-	30	25	-
CAC-Q-P25	-	25	30	-	25
CAC-Q-V25	-	25	30	25	-

Dry components, i.e. cement and aggregates, were homogenized in a laboratory pan mixer for 120 s. The quantity of water was fixed at 10 % in all mixtures. The green mixtures were poured into steel prismatic molds (40×40×160 mm) and then sealed in polyethylene bags to be preserved at  $20 \pm 2^\circ\text{C}$  and  $95 \pm 5\%$  humidity for the following 48 hours. Upon removing molds the samples maintained under the same conditions during the next 5 days. Until 28<sup>th</sup> day, the samples were stored at  $20 \pm 2^\circ\text{C}$  and  $65 \pm 5\%$  humidity.

Fully solidified 28-days-old samples were submitted to thermal treatment in a laboratory furnace at following temperatures: 400°, 600°, 800° and 1000 °C. The rate of heating was 100 °C/h with 2 hours of delay upon reaching the targeted temperature.

### 2.3. Instrumental analyses

Rheology of green samples, i.e. workability (in mm) of green mixture was estimated via slump test using a flow table (ASTM C230). Bulk density (in kg/m<sup>3</sup>) was calculated as a quotient of concrete sample's mass and its volume. Water absorption (in %) was determined from the weight difference between dry and water-saturated samples previously immersed in boiling water for 2 hours. Compressive strength (in MPa) of hardened concrete samples was tested on an Amsler laboratory hydraulic press in accordance with SRPS EN 1015-12:2016. Tests for compressive strength were conducted on halves of experimental prisms (40×40 mm cross-sectional area). Testing was conducted on the 28-days-old solidified samples and on samples after heating at 400°, 600°, 800 ° and 1000 °C.

Differential thermal analysis was conducted on pulverized samples of vermiculite and perlite. The testing temperature range was 25°-1000 °C. Samples were placed in an alumina pan and heated at a constant heating rate of 10 °C/min in a static air flow.

The X-ray diffraction analysis was employed on vermiculite, perlite and pulverized concrete samples. The XRD patterns were obtained on a Philips PW-1710 automated diffractometer using a Cu tube operating at 40 kV and 30 mA. The instrument was equipped with a diffracted beam curved graphite monochromator and a Xe-filled proportional counter. The diffraction data were collected in 2θ Bragg angle range from 4 to 65°, counting for 1 s (qualitative identification) at every 0.02 ° step. The divergence and receiving slits were fixed 1 and 0.1, respectively. The analysis was conducted at 20 °C in a stationary sample holder.

The morphology of non-polished crushed concrete samples was analyzed on a JEOL JSM-6610LV (JEOL, Japan) scanning electron microscope (SEM) connected with an INCA energy-dispersion X-ray analysis unit; EDX analytical system. An acceleration voltage of 20 kV was used. The samples were coated with carbon.

### 3. Results and discussion

The mineral phase compositions of the PC-P65, PC-V65, CAC-P65 and CAC-V65samples after heat treatment at 600 °C are presented in Fig. 3.

The phase composition of the PC-P65 sample (Fig. 3a) is as follows: Ca<sub>3</sub>SiO<sub>5</sub> (C<sub>3</sub>S - alite, JCPDS-49-0442\*), β-Ca<sub>2</sub>SiO<sub>4</sub> (β-C<sub>2</sub>S - belite, JCPDS-49-1673), CaSiO<sub>3</sub> (W - wollastonite, JCPDS-84-0655), SiO<sub>2</sub> (Q - quartz, JCPDS-46-1045), Ca(OH)<sub>2</sub> (CaH - portlandite, JCPDS-72-0156), CaCO<sub>3</sub> (K- calcite, JCPDS-47-1743), Fe<sub>1-x</sub>S (Py - pyrrhotite, JCPDS-75-0601) and Fe<sub>3</sub>O<sub>4</sub> (M - magnetite, JCPDS-89-0951). The most abundant phases were cement minerals alite and belite, and mineral calcite. Quartz was less abundant, while all remaining phases were detected in traces. The crystallinity degree of all present phases was low. Alite and belite, as the main products of Portland cement hydration, accompanied by smaller amounts of portlandite were still present after the heat treatment at 600 °C. Thereby the created hydration-bonds between cement particles in the concrete samples were still active. The reflections corresponding to alite and belite phases had the highest crystallinity (up to 25 arbitrary units – a.u.). These reflections are situated in 25°-35° section, but they are significantly overlapped and superposed with other mineral phases. Wollastonite as a calcium inosilicate mineral (CaSiO<sub>3</sub>) appeared in the mineral phase composition of PC-P65 as a result of limestone (calcite) reactions induced by the increasing temperature. Pyrrhotite, an iron sulfide mineral, is similar to pyrite, however pyrrhotite is weakly magnetic. Its presence is probably related to magnetite.

\*Powder Diffraction File/Cards.Joint Committee on Powder DiffractionStandards (JCPDS), Swarthmore, PA.

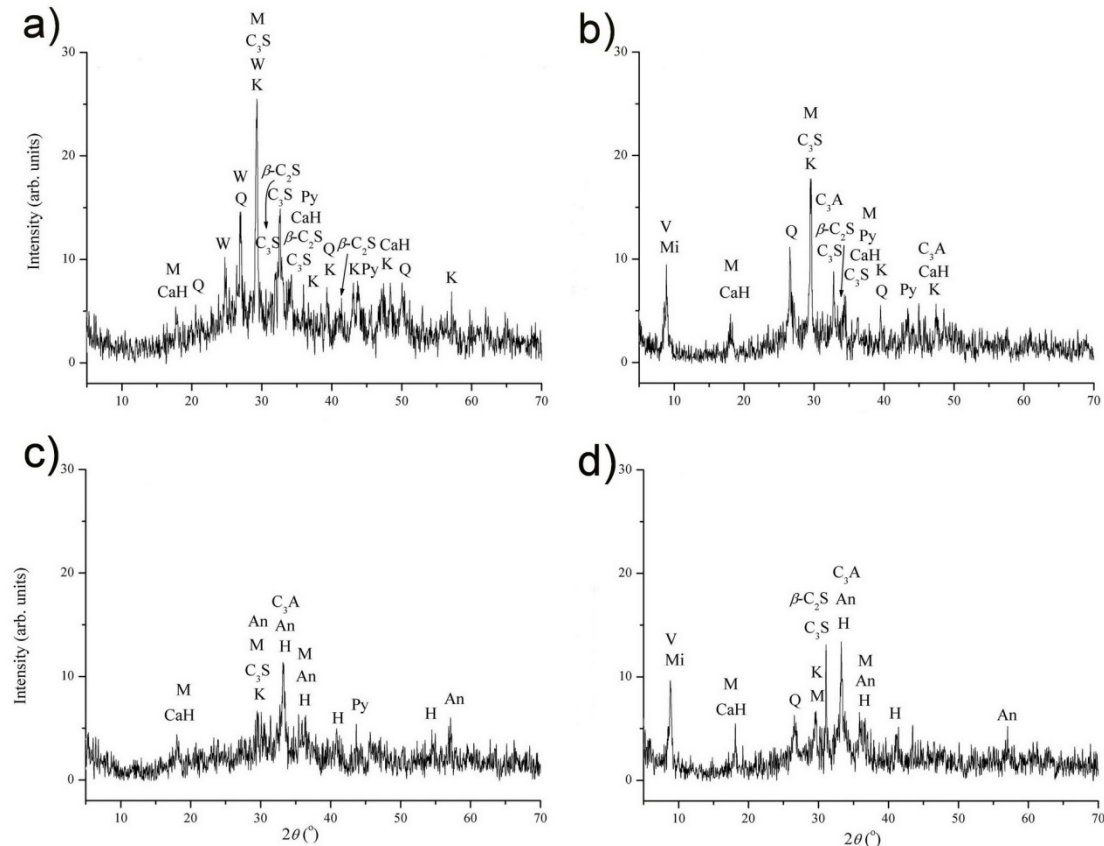


**Fig. 3.** XRD of concrete samples after heat treatment at 600 °C: a) PC-P65; b) PC-V65; c) CAC-P65; d) CAC-V65.

Both Fe minerals were detected in traces, and they can be related to the impurities present in perlite and small quantity of iron oxide present in Portland cement (usually up to 5 %).

In the PC-V65 sample (Fig. 3b) the following mineral phases were identified: alite, belite, tricalcium aluminate ( $\text{C}_3\text{A}$  -  $\text{Ca}_3\text{Al}_2\text{O}_6$ , JCPDS-38-1429), vermiculite (V, JCPDS-16-0613), muscovite (M -  $\text{KAl}_2\text{Si}_3\text{Al}_1\text{O}_{10}(\text{OH})_2$ , JCPDS-06-0263), mica (Mi), quartz, portlandite, calcite, pyrrhotite and magnetite. The most abundant phases were cement minerals, followed by calcite and vermiculite with muscovite, and lesser amounts of quartz. Other phases were hardly traceable. Crystallinity degree of all present phases was extremely low. The crystallinity of the main cement minerals whose reflections were identified in 25°-35° section was lower than in the PC-P65 sample counting up to only 18 a.u. Pyrrhotite and magnetite, formed in reactions that included impurities from vermiculite and  $\text{Fe}_2\text{O}_3$  from Portland cement were present in traces. Vermiculite as a hydrated laminar mineral (aluminum-iron magnesium silicate) was accompanied by muscovite and mica. These minerals originated from the lightweight aggregate used in this concrete.

The sample CAC-P65 (Fig. 3c) comprised refractory cement; therefore the phase composition was slightly different than those of previous two samples. Two cement minerals – alite ( $\text{C}_3\text{S}$ ) and tricalcium aluminate ( $\text{C}_3\text{A}$ ) were the most abundant phases, but their crystallinity was extremely low (10 a.u. in the 25°-35° area). The hydration bonds in the cement were still present at this point. Portlandite and calcite, also originating from the refractory cement, were less abundant. Pyrrhotite and magnetite were hardly traceable, but

$\text{Fe}_2\text{O}_3$  (H - hematite, JCPDS-87-1164) was detected in higher amounts. This can be explained by increased amount of iron oxide in CAC: 16.28 %. Also andradite (An -  $\text{Ca}_3\text{Fe}_2(\text{SiO}_4)_3$ , JCPDS-89-4378) was identified in relatively high quantity. This nesosilicate mineral is characterized by very high hardness (up to 7.5. on Mohs hardness scale).

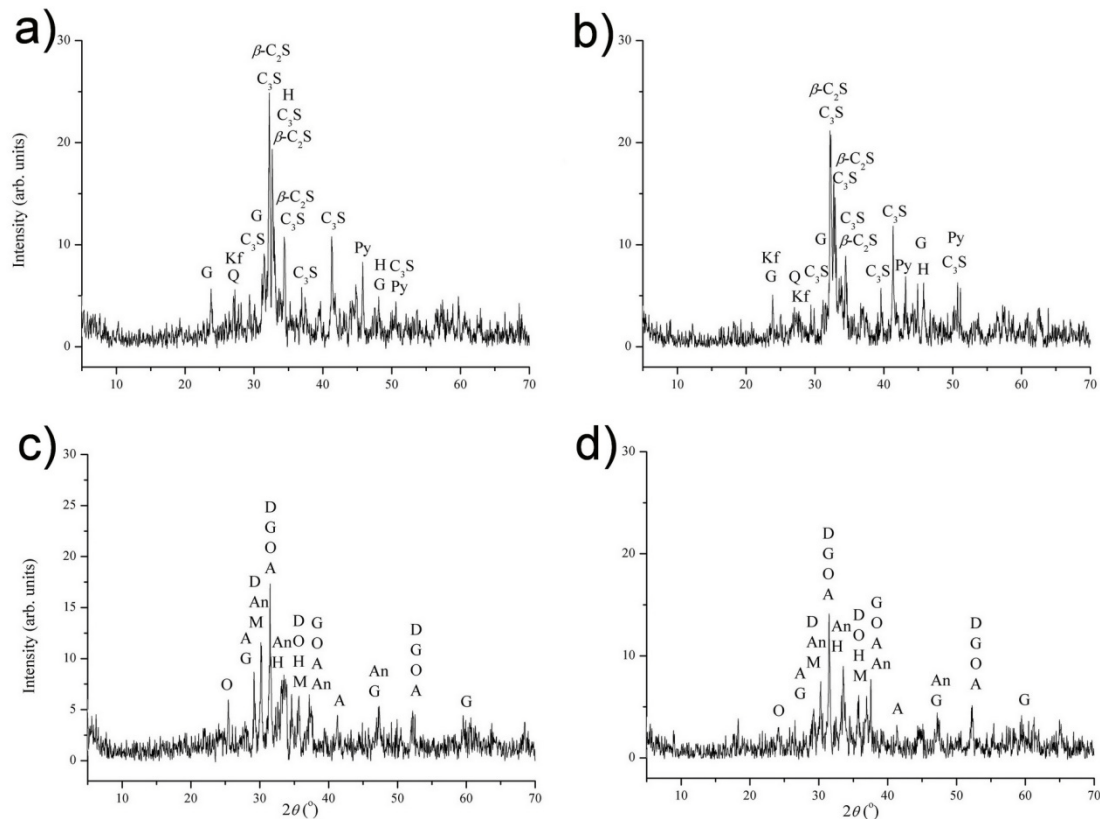


**Fig. 4.** XRD of the concrete samples after heat treatment at 1000 °C: a) PC-P65; b) PC-V65; c) CAC-P65; d) CAC-V65.

The sample CAC-V65 (Fig. 3d) comprised the following mineral phases: alite, belite, tricalcium aluminate, vermiculite, muscovite, quartz, portlandite, calcite, andradite, magnetite and hematite. The cement minerals were matching to those of CAC-P65 regarding their abundance and crystallinity. Andradite was present in this concrete sample, too. The vermiculite and muscovite minerals originated from the lightweight aggregate.

The mineral phase compositions of the samples PC-P65, PC-V65, CAC-P65 and CAC-V65 after heat treatment at 1000 °C are presented in Fig. 4.

Upon heat-treatment at 1000 °C, the majority of hydraulic bonds in cement were replaced by ‘chemical’ bonds. This means that new high temperature mineral phases were created as a result of the concrete sintering. Namely, in the PC-P65 sample (Fig. 4a), alite ( $\text{C}_3\text{S}$ ) and belite( $\beta\text{-C}_2\text{S}$ ) were still present as the most abundant crystalline phases. The intensity of the main alite + belite superposed reflection at 33° was 25 a.u. Quartz and K-feldspar (Kf -  $\text{KAISi}_3\text{O}_8$ , JCPDS-89-1455) were identified in small amounts. Pyrrhotite and hematite were detected in traces. Gehlenite (G -  $\text{Ca}_2\text{Al}_2\text{SiO}_7$ , JCPDS-89-6887) was detected as a new mineral phase. Gehlenite is a sorosilicate with a high melting point: 1593 °C.

The sample PC-V65 (Fig. 4b) had similar mineral phase composition: alite, belite, quartz, gehlenite, K-feldspar, pyrrhotite and hematite. Besides glassy phase, the most abundant crystal phases were cement minerals. All other phases were present in small amounts. The intensity of the main alite + belite reflection at 33° was 20 a.u. Very small

differences between the diffractograms of PC-P65 and PC-V65 samples can be noticed. This suggests that the employed aggregates did not make the prevailing influence on the sintering of concrete; actually the applied cement type proved to be significantly more influential.

The X-ray diffractograms of CAC-P65 and CAC-V65 samples (Fig. 4c, d) showed high similarities. However, the identified mineral phases significantly varied from PC-based samples due to the differences in the sintering mechanisms of Portland cement and calcium aluminate cement. Both CAC-P65 and CAC-V65 comprised: gehlenite as predominant high temperature mineral, andradite and pyroxene/diopside (D - Ca(Mg,Fe)(Si,Al)<sub>2</sub>O<sub>6</sub>, JCPDS-89-0831). Diopside is also characterized by its high melting point (1391 °C). These phases were the most abundant. Less abundant were: olivine (O - (Fe,Mg)<sub>2</sub>SiO<sub>4</sub>, JCPDS-88-2001) and akermanite (A - Ca<sub>2</sub>MgSi<sub>2</sub>O<sub>7</sub>, JCPDS-87-0046). Depending on the amount of forsterite in olivine, its melting point can be as high as 1900 °C. Akermanite is usually associated with gehlenite, and its melting point is approximately 1380 °C. Magnetite and hematite were detected in traces.

The differences in mineral compositions of PC-Q-V25 and CAC-Q-V25 samples upon heating at 600 °C as a result of the applied type of cement are illustrated in Fig. 5.

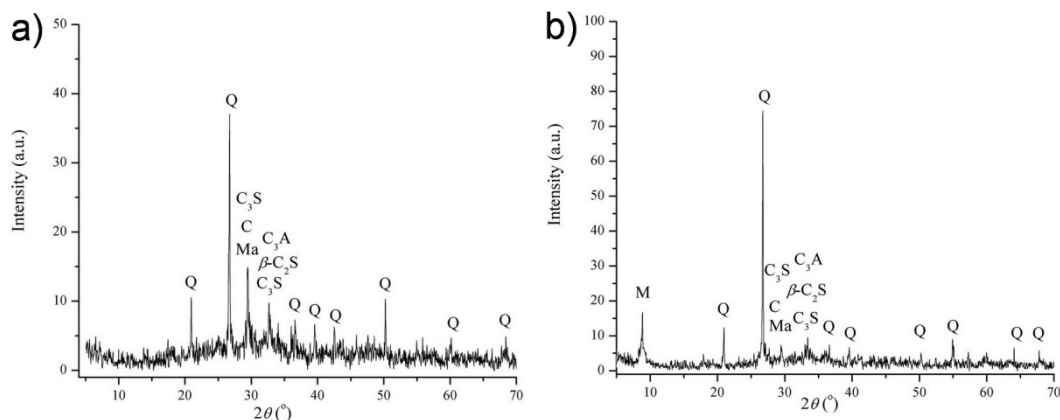


**Fig. 5.** XRD of concrete samples after heat treatment at 600 °C: a) PC-Q-V25; b) CAC-Q-25.

The phase composition of the PC-Q-V25 sample (Fig. 5a) is: alite, belite, tricalcium aluminate, quartz, calcite and magnetite. The most abundant phase was quartz which originated from the prevailing SiO<sub>2</sub> aggregate used in this concrete. Cement minerals are relatively abundant, while all other phases are much lesser present. CAC-Q-V25 sample (Fig. 5b) comprised: alite, belite, tricalcium aluminate, quartz, calcite, muscovite and magnetite. Calcium related phases are comparatively more present in this sample than in PC-Q-V25, due to the higher CaO content in CAC cement.

The XRD diffractograms of the PC-Q-P25, PC-Q-V25, CAC-Q-P25 and CAC-Q-V25 samples upon heating at 1000 °C are given in Fig. 6.

The phase composition of PC-Q-P25 (Fig. 6a) sample: C<sub>3</sub>S - alite, β-C<sub>2</sub>Si - belite, C<sub>3</sub>A, quartz, gehlenite, K-feldspar, Ca<sub>5</sub>(PO<sub>4</sub>)<sub>3</sub>(OH) (apatite, JCPDS-49-0442). Apatite (A) belongs to a group of phosphate minerals with a high melting point (1660 °C). The most abundant phases were quartz and gehlenite, followed by cement minerals. K-feldspar was detected in minor quantities. Apatite was identified in small quantities. The PC-Q-V25 sample with vermiculite aggregate comprised a highly similar mineral phase composition (alite, belite, C<sub>3</sub>A, quartz, gehlenite, K-feldspar, and muscovite) due to the application of the same cement type (Fig. 6b). Upon sintering at 1000 °C, the refractory cement based sample CAC-Q-P25 (Fig. 6c) was composed of the following minerals: alite, belite, C<sub>3</sub>A, quartz, calcite, magnetite, gehlenite, K-feldspar. Quartz and gehlenite were the most abundant phases.

Similarly, the phase composition of CAC-Q-V25 (Fig. 6.d) was  $\text{C}_3\text{A}$ , quartz, calcite, muscovite, gehlenite. Quartz, gehlenite and muscovite were the most abundant phases.

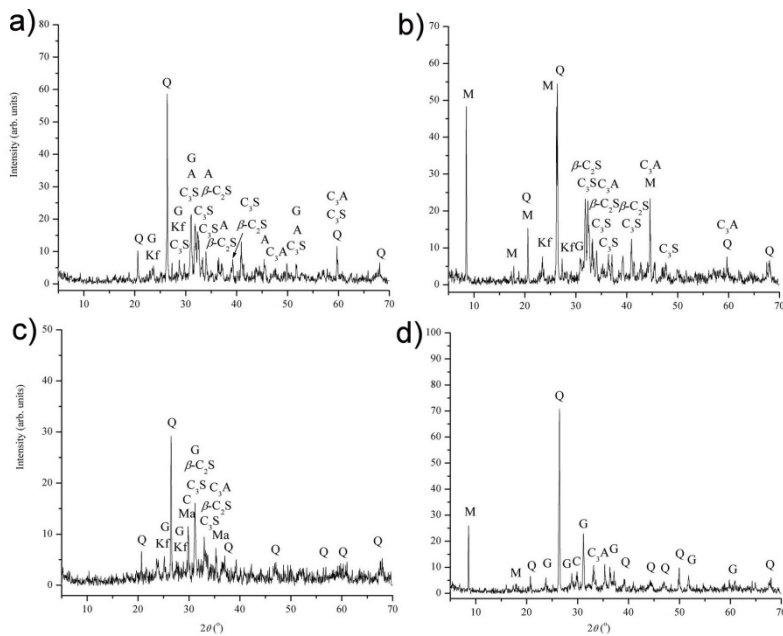


**Fig. 6.** XRD of the concrete samples after heat treatment at 1000 °C: a) PC-Q-P25; b) PC-Q-V25; c) CAC-Q-P25; d) CAC-Q-V25.

It can be noticed that sintering process was governed by the type of cement – whether it is Portland cement or calcium aluminate cement. Impurities originating from the used aggregates might be involved in the reactions, but the quantities of formed mineral phases were low and therefore they could not reduce the quality of the thermal insulation concrete. Upon comparison of the mineral phases present at 600 °C and those identified at 1000 °C, it can be noticed that hydration bond in cement was replaced by chemical bond during this interval which resulted in a number of mineral phases with high melting points.

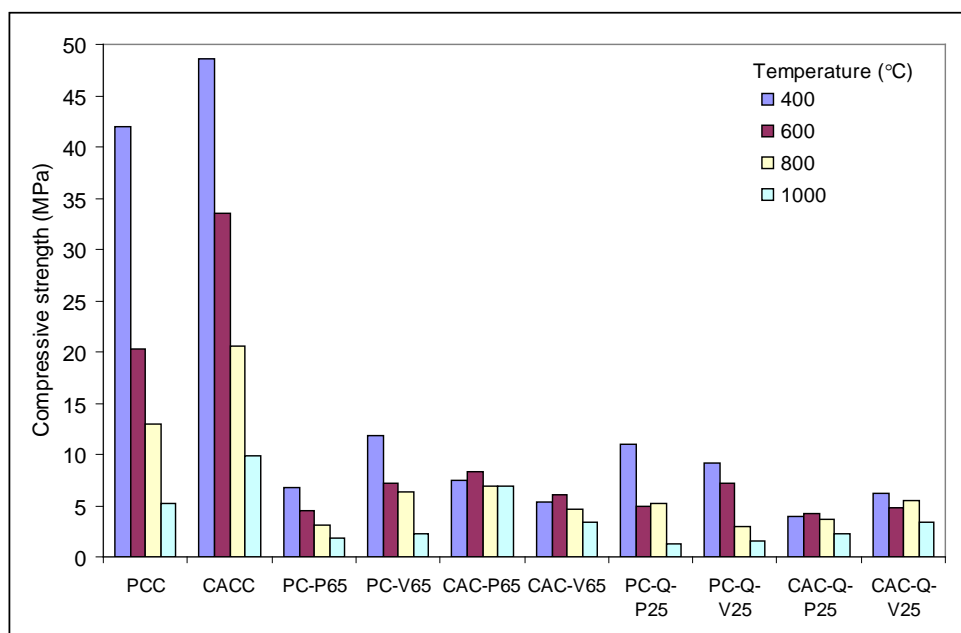
The physico-mechanical properties of the concretes measured/determined at ambient temperature are provided in Tab. III.

**Tab. III** Physico-mechanical properties of the experimental concretes.

Sample	Workability (mm)	Water absorption (%)	Bulk density of green samples (kg/m <sup>3</sup> )	Bulk density of solidified samples (kg/m <sup>3</sup> )	Compressive strength (MPa)
PCC	194	6.92	2350	2225	60.60
CACC	217	7.16	2440	2290	95.70
PC-P65	160	36.20	1490	1450	18.20
PC-V65	143	34.50	1335	1315	9.90
CAC-P65	160	37.20	1480	1455	23.30
CAC-V65	120	46.00	1440	1410	19.06
PC-Q-P25	160	29.06	1530	1500	23.10
PC-Q-V25	140	29.20	1455	1430	20.45
CAC-Q-P25	160	28.53	1520	1475	27.10
CAC-Q-V25	145	27.60	1490	1460	25.30

The consistency (i.e. workability) of the concrete samples that included expanded vermiculite and perlite as aggregates (or aggregate replacements) was drier than consistency of PCC and CACC concretes due to the increased porosity and higher requirements for water. Consequently, PC-P65, PC-V65, CAC-P65 and CAC-V65 exhibited approximately 6 times higher water absorption values in comparison with PCC and CACC. Similarly, PC-Q-P25, PC-Q-V25, CAC-Q-P25 and CAC-Q-V25 had higher water absorptions than PCC and CACC, but the values were lower than those of concretes with the expanded vermiculite or perlite as aggregates. Bulk densities in dry condition (i.e. bulk densities of the solidified samples measured after 28 days) were lower than bulk density of the standard PC concrete. However, all bulk densities were below 1900 kg/m<sup>3</sup>, which categorized these concretes as lightweight. Furthermore, bulk densities being higher than 800 kg/m<sup>3</sup> refer to the fact that the investigated concretes can be used both as insulation materials and structural materials. The complete replacement of standard aggregate with lightweight aggregate influenced a decrease in the 28-days compressive strengths, i.e. compressive strengths of PC-P65 and PC-V65 were 3 and 6 times lower, respectively, than compressive strength of PCC. When refractory cement (CAC) was used in combination with lightweight aggregates, the decrease in compressive strengths was approximately 4.5 times. The concretes with quartz aggregate and expanded vermiculite/perlite as aggregate replacement exhibited 20 % higher compressive strengths than concretes that comprised lightweight aggregate solely.

The decrease in compressive strengths of investigated concretes induced by the increasing temperature is illustrated in Fig. 7. The concrete with perlite aggregate (PC-P65) exhibited a lesser strength deterioration than PC-V65. The compressive strengths of concretes prepared with refractory cement (CAC-P65 and CAC-V65) underwent very small changes with the increasing temperature. The combination PC + quartz aggregate + perlite/vermiculite aggregate replacement exhibited significant decrease in compressive strength, unlike corresponding concretes prepared with refractory CAC cement.

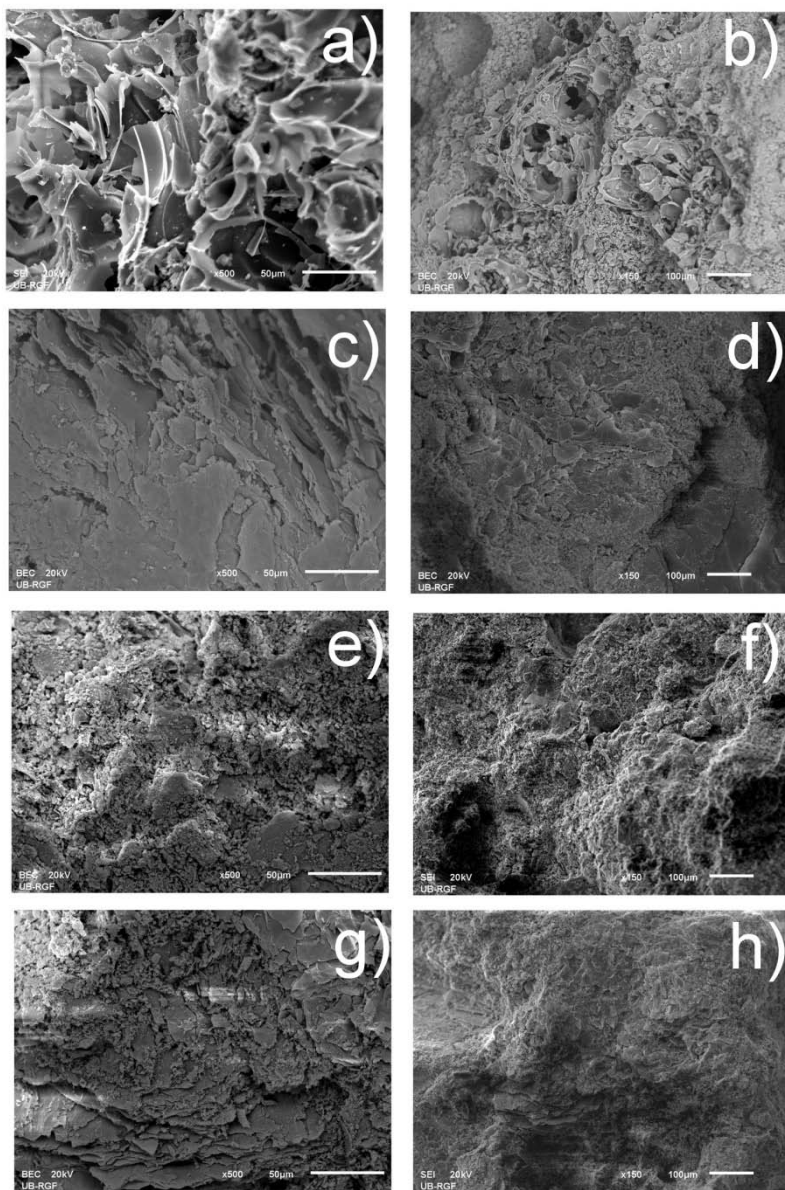


**Fig. 7.** Compressive strengths of concretes determined after firing at 400°, 600°, 800° and 1000°C.

The SEM microphotographs ( $\times 500$  and  $\times 150$  recording magnification) of the samples CAC-P65 and CAC-Q-P25, which showed the smallest compressive strength variations, are provided in Fig. 8. EDX chemical analyses of the concrete samples are given in Tab. IV.

**Tab. IV** EDX chemical analyses of the concretes illustrated in the SEM microphotographs.

Oxide (%)	Al <sub>2</sub> O <sub>3</sub>	SiO <sub>2</sub>	CaO	Fe <sub>2</sub> O <sub>3</sub>	TiO <sub>2</sub>	Na <sub>2</sub> O	K <sub>2</sub> O
CAC-P65 (20°C)	23.10	53.57	11.79	4.93	0.55	2.53	3.16
CAC-P65 (1000°C)	37.54	13.96	32.32	13.22	1.28	0.83	0.85
CAC-Q-P25 (20°C)	18.88	60.82	8.97	4.66	0.40	2.58	3.70
CAC-Q-P25 (1000°C)	41.93	20.94	25.93	8.32	0.63	1.08	1.16

**Fig. 8.** SEM microphotographs of: a and b) CAC-P65 at 20 °C; c and d) CAC-P65 at 1000 °C; e and f) CAC-Q-P25 at 20 °C; g and h) CAC-Q-P25 at 1000 °C.

Two samples of CAC-P65 concrete are compared in Fig. 8a-d. The sample in Fig. 8b is fully hydrated and solidified at ambient temperature. The other sample (Fig. 8d) was recorded upon firing at 1000 °C. In Fig. 8a, a magnified perlite grain is illustrated. The

characteristic lamellar structure of the expanded perlite composed of thin “flakes” can be seen. The crystallinity of perlite is extremely low, as it was showed by XRD analysis (Fig 1b). Thin flakes have an amorphous structure with no pores. However, flakes are aligned into laminas by such leaving the vacant spaces between singular flakes. This lamellar composition represents a base of expanded perlite grain porous structure. In Fig. 8b, a characteristic cluster of several perlite grains is noticed. This section has significantly increased porosity in comparison with the rest of the cementitious sample. In Fig. 8c-d, the structure is more homogenous and characterized by the absence of pores due to the sintering. The structure of the CAC-Q-P25 sample is significantly less porous than CAC-P65. Small inclusions of flaky perlite structures are visible in the microphotographs recorded before and after sintering. The changes in the mineral phase composition (e.g. formation of high temperature phases like gehlenite) previously identified by XRD are highlighted by visible differences in the chemical composition of the samples CAC-P65 and CAC-Q-P25 detected by EDX analyses (Tab. IV) prior to and upon sintering.

#### **4. Conclusion**

Influence of elevated temperature (400-1000 °C) on the mineral phase compositions, microstructure and mechanical properties of thermal insulation concretes was investigated in this study. Two groups of concretes were successfully fabricated: 1) concretes based on the expanded vermiculite or perlite as lightweight aggregates; and 2) concretes based on quartz aggregate with vermiculite or perlite used as the aggregate replacement. Performances have been compared to those of standard-weight concretes based on Portland cement or refractory calcium aluminate cement as binders and quartz aggregate.

The sintering process was governed mainly by the type of cement. Impurities originating from lightweight aggregates were involved in the high-temperature reactions, but the quantities of newly formed mineral phases were scarce. Therefore, the employed aggregates did not make the prevailing influence on the sintering of concrete, instead the applied cement type proved to be significantly more influential. The hydration bonds in cement were replaced by chemical bonds during 600 °-1000 °C interval. At 1000 °C, a number of mineral phases with high melting points were detected (e.g. gehlenite).

The bulk densities of investigated concretes were below 1900 kg/m<sup>3</sup>, which categorized these concretes as lightweight. The complete replacement of standard aggregate with lightweight aggregate influenced a decrease in the 28-days compressive strengths (3-6 times for PC concretes and 4.5 times for concretes with refractory cement). The concretes with quartz aggregate and expanded vermiculite/perlite as aggregate replacement exhibited 20 % higher compressive strengths than concretes that comprised lightweight aggregate solely. The compressive strength of concretes prepared with refractory cement and lightweight aggregate underwent very small changes with the increasing temperature. The results indicated that despite the decrease in compressive strengths upon firing, the investigated lightweight concretes can be categorized both as thermal insulators and structural materials.

#### **Acknowledgments**

This investigation is financially supported by Ministry of Education, Science and Technological Development of the Republic of Serbia.

## 5. References

1. M. Shannag, *Constr Build Mater* 25 (2011) 658.
2. Y.Guruprasad, A. Ramaswamy, *Constr Build Mater* 205 (2019) 549.
3. A. Neville, J. Brooks. *Concrete Technology*. 2nd ed. Prentice Hall (2010).
4. G. Zeer, E. Zelenkova, N. Nikolaeva, et al., *Sci Sint* 50 (2018) 173.
5. P. Trtik et al., *NuclInstrum Meth A* 651 (2011) 244.
6. R. Madandoust, M. Ranjbar , S. Mousavi, *Constr Build Mater* 25 (2011) 3721.
7. M. Zaid, K. Matori et al. *Sci Sint* 49 (2017) 409.
8. A. Schackow, C. Effting, M. Folgueras et al., *Constr Build Mater* 57 (2014) 190.
9. A. Rashad, *Constr Build Mater* 125 (2016) 53.
10. N. Obradović, W. Fahrenholtz, S. Filipović et al., *Sci Sint* 51(2019) 363.
11. P. Gedeonov, *Stroit Mater* 7 (1991) 16.
12. M. Valášková, G. Martynková, B. Smetana, S. Študentová, *Appl Clay Sci* 46 (2009) 196.
13. A. Campos, S. Moreno, R. Molina, *Earth Sci Res J* 13 (2009) 108.
14. S. Chandra, L. Berntsson, *Lightweight Aggregate Concrete*, Noyes Publications/William Andrew Publishing, NY (2002) 367.
15. O. Sengul, S. Azizi, F. Karaosmanoglu, M. Tasdemir, *Energy Build* 43 (2011) 671.
16. S. Erdogan, *J Matern Civil Eng* 27 (2015) DOI: 10.1061/(ASCE)MT.1943-5533.0001172
17. K. Mo, H. Lee, M. Yong, J. Liu, T. Ling, *Constr Building Mater* 179 (2018) 302.
18. O. Gencel, J. Diaz, M. Sutcu et al., *Energy Build.* 70 (2014) 135.
19. S. Abidi, Y. Joliff, C. Favotto, *Compos. B* 92 (2016) 28.
20. M. Sutcu, *Ceram Int* 41 (2015) 2819.
21. S. Chandra, H. Kumar, V. Manikanta, M. Simhachalam, *Int J Innovative Res Sci* 5 (2016) 4106.
22. K. Al-Jabri, A. Hago, R. Taha, A. Alnuaimi, A. Al-Saidy, *J Mater Civil Eng* 21 (2009) 191
23. A.Schackow, C.Effting, M.Folgueras, S.Guths, G.Mendes, *Constr Build Mater* 57 (2014)190.
24. S. Abdul Rahman, G. Babu, *Int. J. Innovative Res Sci Eng Technol* 5 (2016) 2389.
25. M. Karatas, A. Benli, H. Toprak, *Constr Build Mater* 221 (2019) 163.
26. F. Koksal, E. Mutluay, O. Gencel, *Constr Build Mater* 236 (2020) 117789.
27. V. Medri, E. Papa, M. Mazzocchi, et al., *Mater Design* 85 (2015) 266.
28. D. Fodil, M. Mohamed, *Constr Build Mater* 179 (2018) 25.
29. S. Top, H. Vapur, M. Altiner, et al., *J Molec Struc* 1202 (2020) 127236.
30. O. Sengula, S. Azizi, F. Karaosmanoglu, M. Tasdemir, *Energy Build* 43 (2011) 671.
31. L. Wang, P. Liu, Q. Jing, et at., *Constr Build Mater* 188 (2018) 747.
32. A. El Mir, S. Nehme, J. Asad, *Heliyon* 6 (2020) e03165 DOI: 10.1016/j.heliyon.2020.e03165

**Сажетак:** Ова експериментална студија је спроведена са циљем да се истражи утицај повишене температуре на минералошки састав, микроструктуру и механичка својства термоизолационих лако-агрегатних бетона. Прва група експерименталних бетона је спровењена на бази експандираног вермикулита односно експандираног перлита као лаког агрегата (65 %) у комбинацији са стандардним Портланд цементом или ватросталним калијум алюминатним цементом. Пројекат мешавине друге групе бетона садржао је стандардни кварцни агрегат, перлит или вермикулит као замену за агрегат (25 %) и везиво (ПЦ или ЦАЦ). Справљено је укупно 10 мешавина бетона која су потом произведени у форми 40×40×160 mm испитних призми. Узорци

су након стандардне неге и очвршћавања у трајању од 28 дана термички третирани на 400, 600, 800 и 1000 °C. Промене у кристалиничности и минералном фазном саставу настале услед промене температуре су праћене X-ray дифракционом техником. Микроструктурна визуелизација непечених и печених узорака бетона је спроведена помоћу скенинг електронског микроскопа са EDX анализатором. Резултати су указали на чињеницу да, иако долази до смањења притисне чврстоће услед печења, ови лакоагрегатни бетони се могу категорисати и као термички изолатори и као конструкцијони материјали.

**Кључне речи:** Синтеровање; Минералошки састав; CEM; Механичка својства, Конструкциони материјали.

© 2020 Authors. Published by association for ETRAN Society. This article is an open access article distributed under the terms and conditions of the Creative Commons — Attribution 4.0 International license (<https://creativecommons.org/licenses/by/4.0/>).

